ADVANCED MATERIALS

Electroactive Surfactant Designed to Mediate Electron Transfer Between CdSe Nanocrystals and Organic Semiconductors**

By *Delia J. Milliron*, *A. Paul Alivisatos*,* *Claire Pitois*, *Carine Edder*, and *Jean M. J. Fréchet**

Nanocrystals of CdSe have been coated with an electroactive surfactant designed to facilitate their interaction with a matrix of organic semiconductor. The new design allows independent tailoring of solubility and electronic activity. To achieve chemical control of nanocrystals, it is essential to coat them with a monolayer of surfactant. The primary role of the surfactants is to prevent aggregation and it is generally possible to exchange them for other surfactants in order to control the solubility of the coated nanocrystals in a wide variety of solvents and, in turn, their dispersion in a wide range of polymers. The most common and readily accessible surfactants are alkyl thiols, amines, phosphines, phosphine oxides, and carboxylic acids, all of which are electrical insulators with large bandgaps. In many instances, it is desirable to control the dispersion or solubility of a nanocrystal, while simultaneously providing electrical access to its surface. Earlier work[1] has provided an interesting example of surfactant-facilitated electronic interaction, where conduction through a Au nanocrystal film was mediated by conjugated thiols with resonant energy levels, which displaced insulating alkyl thiols.

In optoelectronic devices, semiconductor nanoparticles have been integrated with organic semiconductors to take advantage of their complementary properties. The inorganic semiconductors have greater electron affinities than the organic materials, so charge transfer at the organic–inorganic interface occurs rapidly, provided no insulating monolayer lies at the interface. Integration of semiconductor nanocrystals into light-emitting diodes (LEDs)[2,3] and photovoltaic cells[4,5] can be accomplished by stripping the surfactant from the nanocrystals during film processing, thereby affording direct contact between the nanocrystals and the polymer. However, when using this process, it is difficult to control the detailed morphology and dispersion of nanocrystals within the polymer.[5] In the case of CdS or CdSe and poly(2-methoxy-5-(2′-ethyl-hexyl-oxy)-*p*-phenylenevinylene) (MEH-PPV), a 1.1 nm thick monolayer of the common surfactant, trioctylphosphine oxide (TOPO) located on the surface of the nanocrystals, was sufficient to reduce electron transfer efficiency by a factor of 10.[5] Thus, there is a significant need for a surfactant that can control the dispersion of semiconductor nanocrystals in a wide variety of solvents and polymers, while also permitting electron and hole transfer to organic semiconductors.

Recently, complexes of nanoparticles with electroactive organic molecules, such as viologen and bipyridine derivatives, have been explored as controlled models of the interface between organic and inorganic semiconductors.[6–8] Complex formation with oxide semiconductors benefits from well-established binding methodologies using electrostatic attraction with pH-controlled surface charge, or coordination chemistry with carboxylic acid ligands.[7,9,10] Until now, no such general approaches existed for adding organic functionality to the class of compound semiconductors typified by CdSe. Unlike titanium or tin oxides, the bandgaps of compound semiconductors typically fall in the visible or near-infrared range, making them especially important optoelectronic materials. We now present a general binding strategy for CdSe and apply it to create electroactive oligothiophene surfactants that undergo excited-state charge transfer when complexed to nanocrystals.

Three components of the surfactant must be controlled independently: i) the head group must have a high affinity for CdSe, ii) the electronic levels must have appropriate alignment, and iii) the end groups must provide solubility in a chosen solvent. The most effective head group for functionalization of the colloidal CdSe surface is a phosphonic acid group. Phosphonic acids bind more strongly than amines, thiols, phosphines, and phosphine oxides; it is desirable to incorporate this functionality in the electroactive surfactant and use it to permanently displace these common ligands. Previously, 1,12-diazaperylene was successfully used to displace TOPO with a chromophore.[8] However, the bipyridine moiety, responsible for displacing the TOPO, also plays an integral role in the optical characteristics of this chromophore. In contrast, the phosphonic acid moiety can be used as a distinct binding group with any given chromophore. In this study, the electroactive surfactant we have designed belongs to the family of regioregular 3-hexyl oligothiophenes. Oligothiophenes can be made in a modular way, with controlled conjugation length. By varying the length, energy levels can be adjusted to provide a path for charge transfer. We demonstrate that when the oligothiophenes exceed a critical length, charge transfer occurs between the oligothiophenes and CdSe nanocrystals. Since unsubstituted oligothiophenes have very poor solubility properties, we have introduced alkyl substituents to confer solubility in non-polar solvents. We emphasize, however, that the number and type of solubilizing group can be widely varied.

CdSe nanocrystals about four nanometers in diameter, as estimated from their absorption spectrum and transmission electron microscopy (TEM) imaging, were prepared in TOPO according to published procedures,[12] then washed with methanol to remove excess surfactant. The oligothiophene surfactant T5-PA, **15**, was prepared using the multistep synthesis shown in Scheme 1. Cleavage of the ethyl methyl silane

[*] Prof. A. P. Alivisatos, Prof. J. M. J. Fréchet, D. J. Milliron, Dr. C. Pitois,, Dr. C. Edder
Department of Chemistry, University of California
Berkeley, CA 94720-1460 (USA)
and
Lawrence Berkeley National Laboratory, Materials Sciences Division
Berkeley, CA 94702 (USA)
E-mail: frechet@cchem.berkeley.edu, alivis@uclink4.berkeley.edu

[**] Support of this work by the US Department of Energy under grant DE-AC03-76SF00098 is gratefully acknowledged. D.J.M. thanks the DoD and C.E. thanks the Swiss National Science Foundation for fellowship support. The authors also acknowledge helpful advice on ligand substitution procedures from Dr. Liberato Manna.

  0935-9648/03/0101-0058 $ 17.50+.50/0

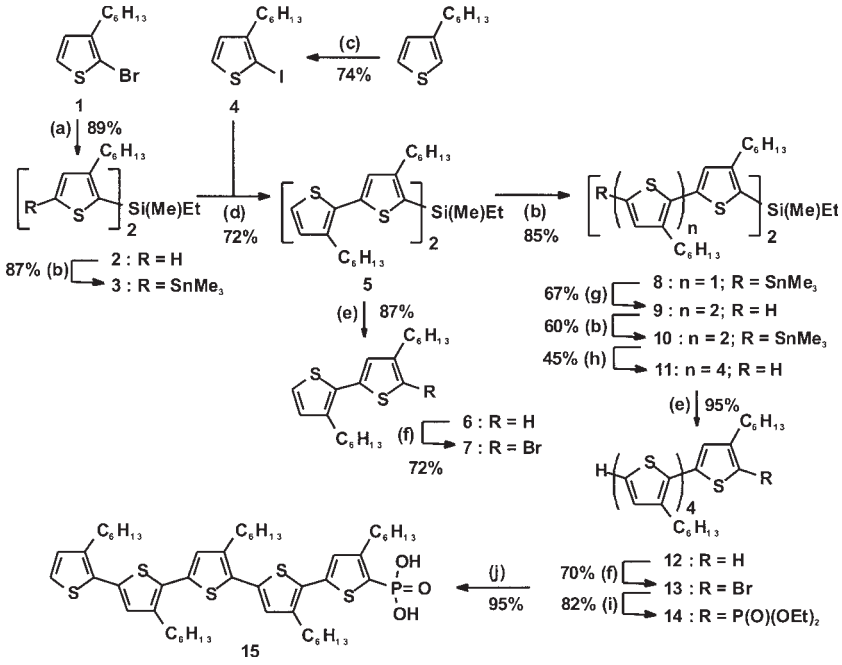

Scheme 1. Preparation of the substituted pentathiophene phosphonic acid T5-PA **15**. a) 1: *n*BuLi, –78°; 2: $Cl_2Si(Me)Et$, –78°. b) 1: N,N,N′,N′-Tetramethylethylenediamine (TMEDA), *n*BuLi –78°; 2: Me_3SnCl, –78°. c) *N*-Iodosuccinimide (NIS). d) $Pd(PPh_3)_2Cl_2$, DMF, 70°. e) Tetrabutylammonium fluoride (TBAF). f) *N*-Bromosuccinimide (NBS). g) **4**, $Pd(PPh_3)_2Cl_2$, dimethylformamide (DMF), 70°. h) **7**, $Pd(PPh_3)_2Cl_2$, DMF, 70°. i) $P(OEt)_3$, $NiCl_2$, 145°. j) 1. $BrSiMe_3$; 2. H_2O.

protecting group of compound **11** with fluoride ion affords two molecules of the regioregular 3-hexyl-substituted pentathiophene **12**, which, after bromination was transformed into the phosphonate ester, **14**, by an Abruzov-type nucleophilic displacement in the presence of nickel chloride.[13,14] Finally, phosphonate **14** was dealkylated and hydrolyzed into the corresponding pentathiophene phosphonic acid (T5-PA), **15**, under mild conditions.[15,16]

Ligand exchange to displace TOPO and create the desired nanocrystal–surfactant complexes was carried out in an inert environment. The nanocrystals and surfactants were co-dissolved in CH_2Cl_2 and allowed to react overnight. The product was precipitated in methanol or ethyl acetate to remove the displaced TOPO and any excess of the new surfactant. Upon redispersion, molecules remain bound to the nanocrystals since the lack of competitive adsorption with TOPO enhances the overall binding constant. ^{1}H NMR analysis of the product in chloroform confirms the binding of the pentathiophene onto the nanocrystals. A comparison of the spectra of free and complexed T5-PA shows both a shift and a broadening of the peaks upon complex formation (see Fig. 1). This broadening results from inhibited molecular rotation as the nanocrystal and its bound molecules rotate together.[17] An estimation of the number of oligothiophene molecules bound to each nanocrystal could be made by deconvoluting the absorption spectra of the complexes and estimating the absorption coefficients for the surfactant molecules and nanocrystals. Typically, the complexes contained about 50 T5-PA molecules per CdSe nanocrystal.

Changes in fluorescence quantum yield indicate differences in the branching ratio between radiative and nonradiative decay and therefore serve as a useful indicator of nanocrystal–oligomer interaction. Quantitative fluorescence yields of the oligomers are determined using an integrating sphere.[18] As the oligothiophenes investigated have higher-energy optical gaps than CdSe nanocrystals (see Fig. 2), both components absorbed the 457 nm excitation light. Therefore, emission and absorption spectra were deconvoluted to determine the molecular fluorescence yields in the complexes. T5-PA dissolved in toluene had a quantum yield of 14.8 %, while CdSe–T5-PA complexes in toluene only had a 1.4 % quantum yield of molecular fluorescence. The exact amount of fluorescence was found to depend on the specifics of the washing procedure used to remove unbound T5-PA molecules, suggesting that this remaining fluorescence could be attributed to remaining unbound T5-PA. Preliminary investigation of a similar pentathiophene (T5) with multiple phosphonic acid groups yielded a similar quenching factor without any washing step. As the remaining molecular fluorescence could be assigned to free molecules, so this result indicates a very high association constant of the multi-ligand chromophore with the nanocrystal surface. Because the T5 emission spectra completely overlap the nanocrystal absorption (Fig. 2), fluorescence quenching upon complexation

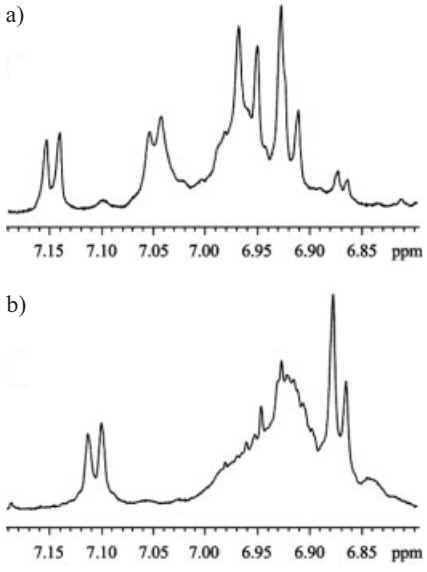

Fig. 1. Aromatic region ^{1}H NMR spectra of pentathiophene **15** (T5-PA) before (a) and after (b) complexation with CdSe nanocrystals. The spectrum of the complex contains broad peaks due to the restricted rotation of T5-PA.

  0935-9648/03/0101-0059 $ 17.50+.50/0

ADVANCED MATERIALS

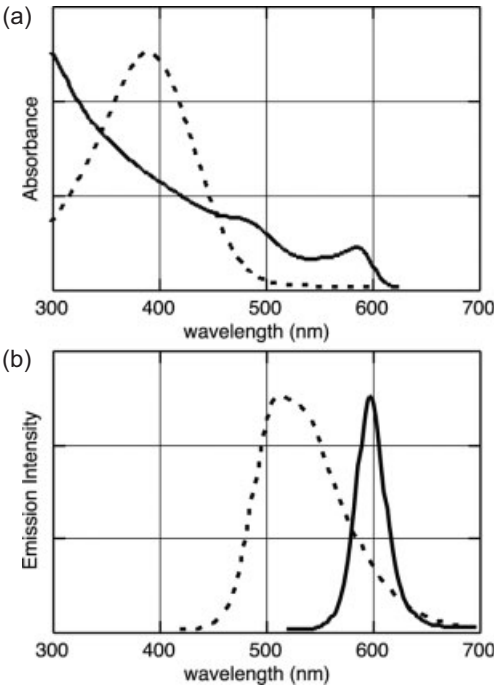

Fig. 2. Absorption (a) and emission (b) spectra of T5-PA and CdSe nanocrystals used in this work.

could result either from electron transfer or energy transfer from excited oligomers to nanocrystals.

Observing the response of the nanocrystal fluorescence yield to bound oligomers resolves the ambiguity of the molecular quenching mechanism. A fixed concentration of nanocrystals was equilibrated with a series of T5-PA concentrations in toluene. As the concentration of T5-PA increased, the fluorescence quantum yield measured after selective excitation of CdSe decreased (Fig. 3). The absolute nanocrystal quantum yield varies from batch to batch, but is typically between one and five percent before complexation with T5-PA. The quenching mechanism requires careful consideration. Energy transfer can be eliminated as a possibility since the optical gap of the oligomer is of substantially higher energy than that of the nanocrystals. Non-passivated surface states provide channels for facile nonradiative decay in CdSe nanocrystals.[19] Hence, changes in surface functionalization can strongly affect fluorescence quantum yields,[20] even in the absence of electroactive components such as oligothiophenes. Using an electronically passive phosphonic acid, phenylphosphonic acid, we observed a slight enhancement in CdSe nanocrystal fluorescence under conditions similar to those used for experiments with T5-PA. The slight increase in quantum yield over that of CdSe capped with only TOPO is consistent with the effective passivation of surface nonradiative decay sites by the phosphonic acid moieties. Variations in the length of the oligothiophene chain were also found to influence nanocrystal fluorescence. A comparison of analogous terthiophene (T3) and pentathiophene (T5) ligands shows that both are quenched by CdSe, but nanocrystal fluorescence increased after complexation with T3 while it decreased with T5. Hence,

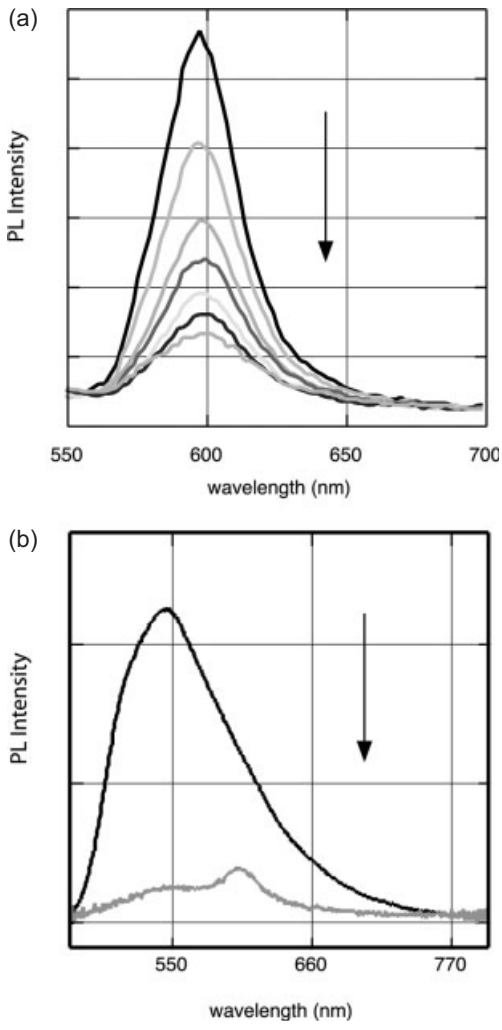

Fig. 3. a) Photoluminescence intensity of CdSe nanocrystals upon addition of T5-PA. Fluorescence of approximately 0.12 μM nanocrystals, selectively excited with 540 nm light, decreased with increasing T5-PA concentration of approximately 0, 1.4, 3.5, 4.3, 5.0, 6.9, and 10.1 μM. b) Photoluminescence of T5-PA before (dark) and after (light) binding to CdSe nanocrystals. The 457 nm excitation light excites both CdSe and T5-PA, and the spectrum after binding contains a contribution from incompletely quenched nanocrystal emission. The integrated intensity of the molecular contribution to the fluorescence is proportional to the molecular quantum yield in each case.

photoexciting bound T3 results in energy transfer to CdSe, whereas photoexciting bound T5 yields charge transfer. Therefore, T5 ligands quench nanocrystal fluorescence by hole transfer after nanocrystal photoexcitation. This implies that the ionization potential of ground state T5 is smaller than the electron affinity of a photoexcited nanocrystal creating overall staggered energy levels (Type II interface, see Fig. 4); the very alignment required in photovoltaic cells to create charge carriers. The larger highest occupied–lowest unoccupied molecular orbital (HOMO–LUMO) gap of T3 reverses the order, creating a level structure in which the energy levels of CdSe are nested between those of T3 (Type I, see Fig. 4). Just like T5, longer oligothiophenes and polythiophenes are expected to form staggered interfaces with CdSe nanocrystals. Having demonstrated hole transfer from photoexcited nano-

  0935-9648/03/0101-0060 $ 17.50+.50/0

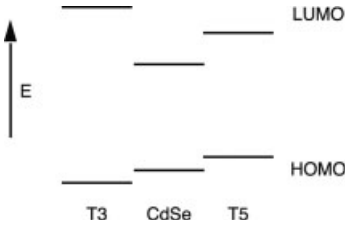

Fig. 4. Schematic of the proposed energy level alignment in CdSe–oligothiophene complexes. Horizontal lines represent the proposed relative energies of the highest occupied and lowest unoccupied electronic energy levels for T3, T5, and CdSe nanocrystals.

crystals to bound T5 ligands, we conclude that molecular excitation results in electron transfer to CdSe, though it may or may not proceed through a nanocrystal excited state. Therefore, when either component in the complex is photoexcited, a charge-separated state results, with a cationic T5 and an anionic nanocrystal.

Oligothiophene–nanocrystal complexes are novel building blocks for solar-cell fabrication. Because oligomers with five rings or more undergo photoinduced charge transfer with nanocrystals, the complexes themselves could serve as the active material in a solar cell. As in CdSe–poly(3-hexylthiophene) (P3HT) solar cells, both components absorb light, and electron transport can be controlled by nanocrystal shape.[4] Unlike in the polymer cells, the interface between T5-PA and CdSe is controlled on a molecular scale. Similarly, it may be possible to create a poly(alkylthiophene) copolymer incorporating functionalities that would provide for more effective mixing with nanocrystals, thereby providing better control of the interface than achievable with standard polymers. Finally, these electroactive surfactants can serve as a third component in nanocrystal–polymer devices by mediating the interaction between the two materials, both physically and electronically. Electronically, a long oligothiophene with phosphonic acid functionality could create a cascade of energy levels between nanocrystals and P3HT. Such a level structure would facilitate forward charge transfer and inhibit recombination by physically separating the electron and hole, as is the case in photosynthesis.

Using phosphonic acid binding groups, we have created soluble oligothiophene–CdSe nanocrystal complexes. Electronic interaction between functional components is facilitated by attaching the binding group directly to the conjugated backbone of the oligomers. We have demonstrated ligand substitution with phosphonic acid groups to be a general strategy for adding organic functionality to CdSe nanocrystal surfaces. Mutual fluorescence quenching of pentathiophene ligands and CdSe nanocrystals indicates photoinduced charge transfer and demonstrates potential utility of these novel materials for the creation of nanocrystal–organic solar cell device structures. The same complexing strategy applies with various oligomers and nanocrystals, selected for their optoelectronic properties, in order to improve both nanocrystal-based photovoltaic cells and LEDs.[21]

Received: September 3, 2002
Final version: October 14, 2002

[1] R. P. Andres, J. D. Bielefield, J. I. Henderson, D. B. Janes, V. R. Kolagunta, C. P. Kubiak, W. J. Mahoney, R. G. Osifchin, *Science* **1996**, *273*, 1690.
[2] H. Mattoussi, L. H. Radzilowski, B. O. Dabbousi, E. L. Thomas, M. G. Bawendi, M. F. Rubner, *J. Appl. Phys.* **1998**, *83*, 7965.
[3] B. O. Dabbousi, M. G. Bawendi, O. Onitsuka, M. F. Rubner, *Appl. Phys. Lett.* **1995**, *66*, 1316.
[4] W. U. Huynh, X. Peng, A. P. Alivisatos, *Adv. Mater.* **1999**, *11*, 923.
[5] N. C. Greenham, X. Peng, A. P. Alivisatos, *Phys. Rev. B* **1996**, *54*, 17 628.
[6] L. Cusack, X. Marguerettaz, S. N. Rao, J. Wenger, D. Fitzmaurice, *Chem. Mater.* **1997**, *9*, 1765.
[7] X. Marguerettaz, A. Merris, D. Fitzmaurice, *J. Mater. Chem.* **1998**, *8*, 2157.
[8] O. Schmelz, A. Mews, T. Basche, A. Herrmann, K. Mullen, *Langmuir* **2001**, *17*, 2861.
[9] M. K. Nazeeruddin, A. Kay, I. Rodicio, R. Humphrybaker, E. Muller, P. Liska, N. Vlachopoulos, M. Grätzel, *J. Am. Chem. Soc.* **1993**, *115*, 6382.
[10] D. A. Gaal, J. T. Hupp, *J. Am. Chem. Soc.* **2000**, *122*, 10 956.
[11] J. B. Ashbury, E. Hao, Y. Wang, H. N. Ghost, T. Lian, *J. Phys. Chem. B* **2001**, *105*, 4545.
[12] X. Peng, J. Wickham, A. P. Alivisatos, *J. Am. Chem. Soc.* **1998**, *120*, 5343.
[13] P. Tavs. *Chem. Ber.* **1970**, *103*, 2428.
[14] I. P. Beletskaya, V. N. Drozd, *Usp. Khim.* **1979**, *48*, 793.
[15] C. E. McKenna, M. T. Higa, N. H. Cheung, M.-C. McKenna, *Tetrahedron Lett.* **1977**, *2*, 155.
[16] Characterization data: **2**: ^{1}H NMR (Bruker AMX-400, 400 MHz, $CDCl_3$): 7.50 (d, J = 5.2 Hz, 2H), 7.04 (d, J = 5.2 Hz, 2H), 2.48 (t, J = 7.8 Hz, 4H), 1.38 (m, 4H), 1.10–1.20 (m, 12H), 1.04 (m, 3H), 0.84 (m, 8H), 0.64 (s, 3H). **3**: ^{1}H NMR: 7.10 (s, 2H), 2.49 (t, J = 7.8 Hz, 4H), 1.35 (m, 4H), 1.02–1.26 (m, 15H), 0.86 (m, 8H), 0.61 (s, 3H), 0.35 (s, 18H). **4**: ^{1}H NMR: 7.39 (d, J = 5.6 Hz, 1H), 6.76 (d, J = 5.6 Hz, 1H), 2.55 (t, J = 7.6 Hz, 2H), 1.55 (m, 2H), 1.32 (m, 6H), 0.90 (t, J = 7.0 Hz, 3H). **5**: ^{1}H NMR: 7.14 (d, J = 5.2 Hz, 2H), 7.06 (s, 2H), 6.92 (d, J = 5.2 Hz, 2H), 2.78 (t, J = 7.8 Hz, 4H), 2.50 (t, J = 7.8 Hz, 4H), 1.10–1.70 (m, 35H), 0.80–0.90 (m, 14H), 0.67 (s, 3H). **6**: ^{1}H NMR: 7.14 (d, J = 5.2 Hz, 1H), 6.94 (d, J = 1.5 Hz, 1H), 6.92 (d, J = 5.2 Hz, 1H), 6.88 (d, J = 1.5 Hz, 1H), 2.74 (t, J = 7.7 Hz, 2H), 2.57 (t, J = 7.7 Hz, 2H), 1.30–1.64 (m, 16H), 0.88 (m, 6H). **7**: ^{1}H NMR: 7.15 (d, J = 5.2 Hz, 1H), 6.91 (d, J = 5.2 Hz, 1H), 6.78 (s, 1H), 2.69 (t, J = 7.6 Hz, 2H), 2.53 (t, J = 7.6 Hz, 2H), 1.30–1.58 (m, 16H), 0.88 (m, 6H). **8**: ^{1}H NMR: 7.02 (s, 2H), 6.98 (s, 2H), 2.77 (t, J = 7.8 Hz, 4H), 2.46 (t, J = 7.8 Hz, 4H), 1.62 (m, 4H), 1.02–1.43 (m, 31H), 0.90 (m, 12H), 0.81 (m, 2H), 0.67 (s, 3H), 0.36 (s, 18H). **9**: ^{1}H NMR: 7.18 (d, J = 5.2 Hz, 2H), 7.11 (s, 2H), 6.96 (s, 2H), 6.94 (d, J = 5.2 Hz, 2H), 2.80 (m, 8H), 2.53 (m, 4H), 0.80–0.95 (m, 20H), 1.10–1.80 (m, 51H), 0.70 (s, 3H). **10**: ^{1}H NMR: 7.06 (s, 2H), 6.99 (s, 2H), 6.93 (s, 2H), 2.77 (m, 8H), 2.49 (m, 4H), 1.05–1.65 (m, 51H), 0.90 (m, 20H), 0.65 (s, 3H), 0.38 (s, 18 H). **11**: ^{1}H NMR: 6.90–7.20 (m, 12H), 2.50–2.80 (m, 20H), 1.20–1.75 (m, 85H), 0.75 (m, 30H), 0.67 (m, 3H). **12**: ^{1}H NMR: 7.16 (d, J = 5.2 Hz, 1H), 6.90–7.05 (m, 6H), 2.80 (m, 8H), 2.60 (m, 2H), 1.70 (m, 10H), 1.40 (m, 30H), 0.90 (m, 15H). **13**: ^{1}H NMR: 7.15 (d, J = 5.2 Hz, 1H), 6.93 (m, 4H), 6.81 (s, 1H), 2.70 (t, J = 7.8 Hz, 2H), 2.75–2.79 (m, 6H), 2.56 (t, J = 7.8 Hz, 2H), 1.60 (m, 10H), 1.30 (m, 30H), 0.90 (m, 15H). **14**: ^{1}H NMR: 7.15 (d, J = 5.2 Hz, 1H), 6.90–7.06 (m, 5H), 4.16 (m, 4H), 2.60–2.90 (m, 10H), 1.68 (m, 10H), 1.24–1.40 (m, 36H), 0.90 (m, 15H). ^{31}P NMR: 11.28 (s). **15**: ^{1}H NMR: 7.15 (d, J = 5.2 Hz, 1H), 6.90–7.06 (m, 5H), 2.60–2.90 (m, 10H), 1.68 (m, 10H), 1.24–1.40 (m, 30H), 0.85 (m, 15H). ^{31}P NMR (Bruker AMX-400, 162 MHz, $CDCl_3$): 17.82 (s). High-resolution mass spectrometry (fast atom bombardment) (Micromass ZAB2-EQ): m/z Calcd for $C_{50}H_{73}O_3PS_5$: 912.3901; Found: 912.3921.
[17] J. R. Sachleben, E. W. Wooten, L. Emsley, A. Pines, V. L. Colvin, A. P. Alivisatos, *Chem. Phys. Lett.* **1992**, *198*, 431.
[18] N. C. Greenham, I. D. W. Samuel, G. R. Hayes, R. T. Phillips, Y. A. R. R. Kessener, S. C. Moratti, A. B. Holmes, R. H. Friend, *Chem. Phys. Lett.* **1995**, *241*, 89.
[19] V. I. Klimov, *J. Phys. Chem. B* **2000**, *104*, 6112.
[20] X. Peng, M. C. Schlamp, A. V. Kadavanich, A. P. Alivisatos, *J. Am. Chem. Soc.* **1997**, *119*, 7019.
[21] N. Tessler, V. Medvedev, M. Kazes, S. Kan, U. Banin, *Science* **2002**, 295, 1506.

  0935-9648/03/0101-0061 $ 17.50+.50/0